

# The distance fluctuation criterion for melting: Comparison of square-well and Morse potential models for clusters and homopolymers

Yaoqi Zhou

*Department of Chemistry and Chemical Biology, Harvard University, Cambridge, Massachusetts 02138 and  
Department of Physiology/Biophysics, SUNY Buffalo, Buffalo, New York 14214*

Martin Karplus<sup>a)</sup>

*Department of Chemistry and Chemical Biology, Harvard University, Cambridge, Massachusetts 02138 and  
Laboratoire de Chimie Biophysique, Institut le Bel, Université Louis Pasteur, 4, Rue Blaise Pascal,  
67000 Strasbourg, France*

Keith D. Ball

*Department of Pharmaceutical Chemistry, University of California at San Francisco, San Francisco,  
California 94118*

R. Stephen Berry

*Department of Chemistry and The James Franck Institute, The University of Chicago, Chicago,  
Illinois 60637*

(Received 19 June 2001; accepted 18 October 2001)

We explore the distance fluctuation criterion (“Lindemann criterion”) for melting transitions. Distances from average positions in accord with Lindemann, or interparticle distances, in accord with Jellinek and Berry or Etters and Kaelberer, are examined. The primary goal is to determine which of these offers the more useful criterion. The choice of origin can sometimes effect the significance of the index. We study three systems with two kinds of potentials. They are all composed of 64 particles: (a) and (b), a homopolymer and a cluster that consist of beads interacting pairwise through square-well potentials, and (c) a cluster of particles interacting pairwise through Morse potentials. For each of the noncrystalline structures, in contrast to the crystals originally studied by Lindemann, the fluctuation parameter based on interparticle distances gives a clearer separability of liquid and solid phases than that based on fluctuations from average positions. The solid-like forms of the Morse cluster, the square-well cluster, and the square-well homopolymer have similar behavior, indicating that a broad class of systems can be evaluated with this index. In these systems, relative fluctuation parameters provide a suitable criterion for the melting transition. The critical values for the interparticle distance criterion, which are in the range of 0.03–0.05, are smaller than those for the Lindemann criterion (0.1–0.15). © 2002 American Institute of Physics. [DOI: 10.1063/1.1426419]

## I. INTRODUCTION

Empirical rules<sup>1–4</sup> have long been used to characterize the melting transitions of solids and have been found to be very useful for identifying the onset of the melting and freezing transition in computer simulations without performing free-energy calculations. Such rules are particularly important because a complete “*ab initio*” theory for the melting transition is not available.<sup>5</sup> The Lindemann criterion, introduced in 1910,<sup>1</sup> measures the atomic vibrational amplitude  $\langle \Delta r^2 \rangle^{1/2}$  in units of the lattice constant  $a$  of a crystal. If this ratio, which is defined as the disorder parameter,  $\Delta_L$ , reaches a certain value, it is presumed that fluctuations cannot increase without damaging or destroying the lattice. Experiments and simulations show that the critical value of  $\Delta_L$  for simple solids is in the range of 0.10–0.15. The critical value has been found to be relatively independent of the types of substance, the nature of the interaction potential, and the crystal structure.<sup>5,6</sup> The criterion has been applied to

study solid-versus-liquid behavior in infinite systems ranging from crystals,<sup>6</sup> such as rare-gas solids, metals, and alkali halides to model systems,<sup>5</sup> such as hard spheres<sup>7</sup> and Yukawa spheres.<sup>8</sup> It has also been used in finite systems, such as clusters,<sup>9</sup> isolated homopolymers,<sup>10</sup> heteropolymers,<sup>11</sup> and proteins.<sup>12</sup>

For irregular finite systems such as rare-gas clusters, an alternative criterion, which we call the distance-fluctuation criterion, has been introduced in two slightly different forms.<sup>13–16</sup> One is based on the Berry parameter  $\Delta_B$ , defined as<sup>16</sup>

$$\Delta_B = \frac{2}{N(N-1)} \sum_{i < j} \frac{\sqrt{\langle \Delta r_{ij}^2 \rangle}}{\langle r_{ij} \rangle}, \quad (1)$$

and the other is the similar Etters–Kaelberer parameter  $\Delta_{EK}$  (Refs. 13–15) defined as

$$\Delta_{EK} = \frac{1}{NP} \sum_{i=1}^{NP} \frac{\sqrt{\langle \Delta r_{ij}^2 \rangle}}{\langle r_{ij} \rangle}, \quad (2)$$

<sup>a)</sup>Electronic mail: marci@tammy.harvard.edu

where  $r_{ij}$  is the distance between atoms  $i$  and  $j$ ,  $\langle \Delta r_{ij}^2 \rangle = \langle (r_{ij} - \langle r_{ij} \rangle)^2 \rangle$ ,  $N$  is the number of particles, and NP is the number of neighboring pairs, where members of each pair are separated by less than a nearest-neighbor cutoff distance  $r_{\text{nn}}$ . The key difference between  $\Delta_B$  (or  $\Delta_{\text{EK}}$ ) and  $\Delta_L$  is that the former is based on the fluctuation of the distance between pairs of atoms while the latter is based on the fluctuation of an individual atom relative to its average position. The critical value of  $\Delta_B$  ( $\Delta_{\text{EK}}$ ) for the liquid–solid transition of finite clusters (above which the value rises rapidly and the system is liquid-like), has been suggested to be almost 0.1,<sup>16–19</sup> similar to the value of  $\Delta_L$ . This may be a reason why the distance-fluctuation criterion is often loosely referred to as the Lindemann criterion in the literature.<sup>16–23</sup> The existence of a surface-molten solid phase in finite systems such as Lennard-Jones clusters,<sup>24–26</sup> square-well clusters,<sup>10</sup> and square-well polymers<sup>10</sup> suggests that a more detailed examination and comparison of these criteria for the liquid–solid transition is appropriate.

In this paper, we examine these fluctuation criteria for the liquid-to-solid transition in model systems with two kinds of potentials. The systems all consist of 64 particles: (a) a homopolymer and (b) a cluster, both of whose particles interact pairwise through a discontinuous square-well potential, and (c) a cluster of particles interacting pairwise through Morse potentials. This range of systems and potentials was used to determine the robustness of the criteria to the choice of system. The systems are small enough for detailed analyses by simulations and large enough to have a well-defined core. The results demonstrate that the criterion based on the distance fluctuations ( $\Delta_B$  or  $\Delta_{\text{EK}}$ ) has critical values smaller than that based on rms fluctuations ( $\Delta_L$ ), and provides a somewhat sharper criterion for melting in these systems.

## II. METHODS

### A. Systems with a square-well potential

A cluster of 64 square-well beads and a freely jointed homopolymer chain of 64 beads are simulated using the discontinuous molecular dynamics technique in a canonical ensemble. The beads interact with each other via a square-well potential that has a hard-core diameter  $\sigma$ , a square-well diameter  $1.5\sigma$ , and square-well depth  $\epsilon$ . Constant-temperature discontinuous molecular dynamics simulations are performed at the reduced temperature  $T^* = k_B T / \epsilon = 0.33$  for the homopolymer chain and 0.29 for the cluster; these are the temperatures at which a liquid-like phase and a surface-molten solid phase coexist.<sup>10,27</sup> We focus on the melting transition of the solid core in both the chains and the clusters. Each simulation starts at a high temperature ( $T^* = 1.0$  or 0.7) and gradually decreases to the target temperature in 150 million collisions. The system is then equilibrated for 100 million collisions and simulated for an additional 250 million collisions to obtain equilibrium averages. The internal energy of the system for the last 250 million collisions is monitored to extract the equilibrium average for each state separately, when they are in equilibrium (see the following). The simulation procedure has been shown to give accurate equilib-

rium thermodynamic results in earlier work.<sup>10,27</sup> Details of the cluster and chain models and the simulation methods are presented there.

To obtain a clear picture of the meaning of  $\Delta_B$  ( $\Delta_{\text{EK}}$ ) in finite systems, it is useful to calculate them as functions of the distance from the center. The distance-dependent Berry parameter can be defined as

$$\Delta_B(r_{\text{cut}}) = \frac{2}{N_{r_{\text{cut}}}(N_{r_{\text{cut}}} - 1)} \sum_i \frac{\sqrt{\langle r_{ij}^2 \rangle - \langle r_{ij} \rangle^2}}{\langle r_{ij} \rangle}, \quad (3)$$

where the summation is only over the  $N_{r_{\text{cut}}}$  atoms (or beads) that are located within a sphere around the center of mass with a radius equal to  $r_{\text{cut}}$ . A similar definition for  $\Delta_{\text{EK}}(r_{\text{cut}})$  can be made where the summation is only over the number of neighboring pairs,  $NP_{r_{\text{cut}}}$ , that are located within a sphere around the center of mass with a radius equal to  $r_{\text{cut}}$ . For a sufficiently large  $r_{\text{cut}}$ , the sphere will enclose all atoms of the system and  $\Delta_B(r_{\text{cut}})$  [ $\Delta_{\text{EK}}(r_{\text{cut}})$ ] becomes equal to  $\Delta_B$  ( $\Delta_{\text{EK}}$ ) for the entire system. The average distance of each bead from the center can be obtained via averaging over equilibrium configurations. In this paper, only results based on  $\Delta_B(r_{\text{cut}})$  are presented because the results based on  $\Delta_{\text{EK}}$  are essentially the same.

For comparison, one can also define a distance-dependent Lindemann parameter

$$\Delta_L(r_{\text{cut}}) = \frac{1}{\sigma} \sqrt{\sum_i \Delta r_i^2 / N_{r_{\text{cut}}}}, \quad (4)$$

where  $\Delta r_i^2 = \langle r_i^2 \rangle - \langle r_i \rangle^2$  with  $\mathbf{r}_i$ , the position of bead  $i$ . The average position is obtained from the simulation after the translations and rotations of all configurations with respect to the first configuration are removed by shifting the center of mass coordinates to the origin and minimizing the root mean-squared deviation by a finite rotation.<sup>28</sup> An advantage of the  $\Delta_B$  and  $\Delta_{\text{EK}}$  parameters is that they require no such superposition.

### B. System with a Morse potential

To test the fluctuation parameter values for more realistic potentials, we select the  $M_{64}$  system, a cluster of 64 particles bound by pairwise Morse interactions

$$V(r_{ij}) = \epsilon \{ [1 - \exp(-\beta(r_{ij} - r_0))]^2 - 1 \}, \quad (5)$$

where  $\epsilon$  is the potential depth,  $\beta$  is the interaction range scaling parameter,  $r_{ij}$  is the distance between particles  $i$  and  $j$ , and  $r_0$  is the minimum-energy pairwise separation. This potential can be expressed in terms of a dimensionless variable  $\rho = \beta r$  and a single parameter  $\rho_0 = \beta r_0$  that characterizes the interaction range of the potential.<sup>29</sup>

The Morse potential was chosen, rather than the more frequently studied Lennard-Jones (LJ) potential, because the latter is, when expressed in dimensionless units, a parameter-free potential, while the Morse potential has one free parameter. Because of this flexibility, the Morse potential has been used in many studies of interaction-range effects on the structure and dynamics on potential energy surfaces.<sup>29–34</sup> When the free parameter ( $\rho_0$ ) is set to a value 6, the Morse

potential has the same curvature at its minimum as that of the Lennard-Jones potential, and the properties of systems with this value of the Morse parameter and systems with Lennard-Jones interactions are very similar.<sup>30</sup> (We will extend this study to other values of  $\rho_0$  in a future paper.) For  $n=55$ , both have the same ground-state structures and similar thermodynamics.<sup>35,36</sup> Hence, we expect the fluctuation properties of  $M_{64}$  with  $\rho_0=6$  to be comparable to those of  $LJ_{64}$ . To generalize the results, we represent all energies in units of  $\epsilon$  and consider the reduced distances  $r/\sigma$ , where  $\sigma=2^{-1/6}r_0$  as defined in the LJ potential.

For the simulations, we employ the stochastic collision constant-temperature molecular dynamics (MD) method of Kast *et al.*<sup>37,38</sup> with modifications suggested by Sholl and Fichthorn,<sup>39</sup> using a time step of  $\tau=2$  fs. As in the case of the square-well systems, the melting transition temperature  $T_{\text{melt}}^*$  is defined as the temperature at which the free energies of the solid and liquid forms are equal, and hence the temperature at which the cluster spends equal time in each of the two forms. We use molecular dynamics simulations to pinpoint  $T_{\text{melt}}^*$  by determining the occupation levels of both liquid-like and surface-melted regions on the potential energy surface and from phase change indicators observed in the caloric curves and heat capacities. From these data we have determined the melting transition temperature of  $M_{64}$  to be  $T_{\text{melt}}^*=0.29$  in reduced units. We measure the mean fluctuation parameters of  $M_{64}$  at  $T_{\text{melt}}^*$  for a series of MD simulations. In each run we first equilibrate the system for  $2 \times 10^6 \tau$ , and then simulate a trajectory with a preselected length ranging from  $2$  to  $8 \times 10^7 \tau$ .

To determine the phase-like form of the system at any given time, one need simply determine the structure of the local minimum (or “inherent structure”<sup>40</sup>) in whose basin of attraction the system trajectory currently dwells. We use the term “phase-like” to indicate a solid-like, surface-molten, or liquid-like phase of the cluster, since the traditional definition of thermodynamic phases applies only to bulk systems. There are some significant differences in the phase behavior of finite systems, such as a “rounding” of discontinuities in first-order phase transitions.<sup>41</sup> In our simulations, the local minima are found by quenching the cluster every  $1000\tau$  via conjugate gradient local minimizations of the potential energy. Phase identification is established by determining a unique range, or band, of quenched potential energy for each phase-like form. We have identified quenched-energy bands for three phases: solid, surface-melted solid (SM), and liquid-like phases. This technique has been used previously in studies of the geometrically similar  $LJ_{55}$  cluster,<sup>26,42–44</sup> in which similar phase-specific energy bands were found.

Once the phase of the cluster has been established, we set  $\mathbf{r}_{\text{c.m.}}=0$  to eliminate cluster translations, and employ the Kabsch least-squares rotation procedure before measuring fluctuation data to minimize the error in calculations of  $\Delta_L$ . We then accumulate the atomic pair separations  $r_{ij}$  and the radial distances  $r_i$  from the origin, as well as the squares of these quantities, in order to determine their averages and mean square deviations.

Since our goal is to evaluate the mean fluctuations for specific phases, we average the mean displacement  $\langle \mathbf{r}_i \rangle$  of

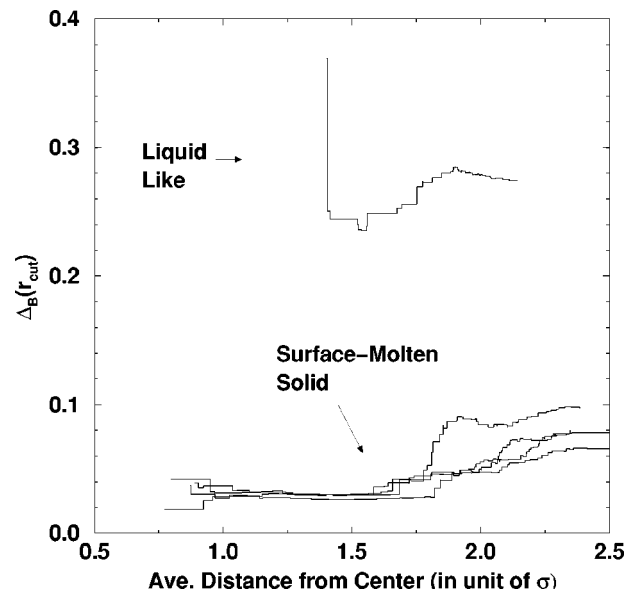


FIG. 1. The distance-dependent Berry parameter,  $\Delta_B(r_{\text{cut}})$ , for an isolated square-well 64mer at  $T^*=0.33$ . The results of five independent runs are shown. Note that the number of particles within  $r < r_{\text{cut}}$  cumulatively increases and the largest  $\Delta_B(r_{\text{cut}})$  value corresponds to the  $\Delta_B$  value for the entire system. The value changes in a stepwise pattern since  $\Delta_B(r_{\text{cut}})$  only changes its value after a new bead is included.

each particle from the center of mass and the mean pair distances  $\langle r_{ij} \rangle$  over trajectory segments in the simulations for which the phase remains unchanged. Such *phase segments* are recorded only if they endure at least 100 quenches ( $10^5 \tau$ ). We used segments, rather than the whole trajectory, because unlike the simulations of square-well systems, along the  $M_{64}$  trajectories, the system passes moderately frequently between phases, and when it returns from liquid to solid, it may end up in some permutational isomer of its previous solid structure. This complication is not unexpected in a phase coexistence region. In Sec. III, we identify the minimum length of a phase segment needed to give statistically reliable values of the fluctuation parameters.

### III. RESULTS

#### A. Systems with a square-well potential

The distance-dependent  $\Delta_B(r_{\text{cut}})$  was calculated for a cluster of 64 beads and for a freely jointed homonuclear 64mer. In Fig. 1,  $\Delta_B(r_{\text{cut}})$  is plotted as a function of average distance from the center of mass for the square-well 64mer. The results from five independent runs at  $T^*=0.33$  show two states in coexistence. The liquid state has a large overall value of  $\Delta_B(\sim 0.27)$  associated with the greater motional freedom resulting from the larger average distance of atoms from the center ( $>1.4 \sigma$ ). The other state has a small near-constant value of  $\Delta_B(\sim 0.03)$  up to  $r=1.75\sigma$ . This corresponds to a solid core that consists of about 20 beads. It is not surprising that beads in liquid-like states have much larger average distances from the center because each bead can move relatively freely between core and surface in the liquid form.

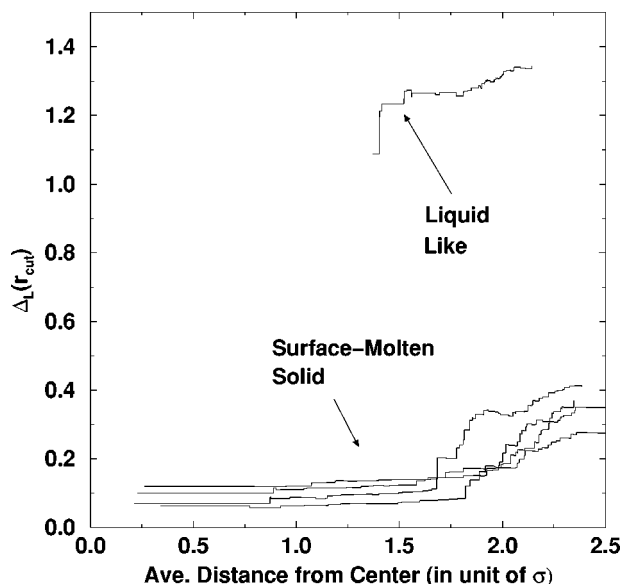


FIG. 2. As in Fig. 1 but for the distance-dependent Lindemann parameter,  $\Delta_L(r_{\text{cut}})$ . The value of  $\Delta_L(r_{\text{cut}})$  starts from the closest bead to the center since it is a criterion based on individual beads. On the other hand,  $\Delta_B(r_{\text{cut}})$  in Fig. 1 starts from the second closest bead to the center since the criterion involves at least two beads.

For larger distances ( $r_{\text{cut}} > 1.75\sigma$ )  $\Delta_B(r_{\text{cut}})$  increases to a value between 0.06 and 0.1, suggestive of a partly molten state. It is not certain whether this phase-like form of the square-well cluster is analogous to the surface-molten state of the Morse and Lennard-Jones cluster, but indications are that the two are similar. (The “surface-molten” phase of Lennard-Jones and Morse clusters have been shown to be rather different from the model of a chaotic layer around an ordered solid core.<sup>42,43</sup>) In any case, the partly molten state of this system is more like a liquid confined to a solid surface than like a homogeneous soft solid, and thus has a  $\Delta_B$  or  $\Delta_L$  value smaller than that of the bulk liquid. Use of a total  $\Delta_B$  value of about 0.1 as the critical value for the transition gives meaningful results since  $\Delta_B$  for the entire system jumps from 0.06–0.1 for the lower state to  $>0.25$  for the upper (liquid) state. However, since the surface is not really solid-like, the true critical value (or threshold limit) for the melting transition is  $\Delta_B \sim 0.03$ – $0.04$ , associated with the value for the solid core. This method of obtaining the critical value is supported by the results of the distance-dependent Lindemann parameter shown in Fig. 2. Based on the  $\Delta_L$  value for the entire system, one would suggest that the critical value is somewhat above 0.3. The  $\Delta_L(r_{\text{cut}})$  value for the solid core (0.12–0.13), however, is more consistent with earlier estimates for other bulk systems<sup>5,6</sup> and finite LJ clusters.<sup>9</sup>

Similar results are obtained for the square-well cluster of 64 beads. Figure 3 shows that the  $\Delta_B(r_{\text{cut}})$  value is nearly a constant (0.02–0.03) for the interior of the solid-like cluster before it undergoes a sudden increase due to surface motions. The surface motions of the cluster, which has fewer constraints than the chain (Fig. 1), are considerably larger and more liquid-like. For the liquid-like phase the average distances of beads from the center cover a much narrower range ( $1.8\sigma < r < 2.1\sigma$ ) than those in the surface-molten solid phase

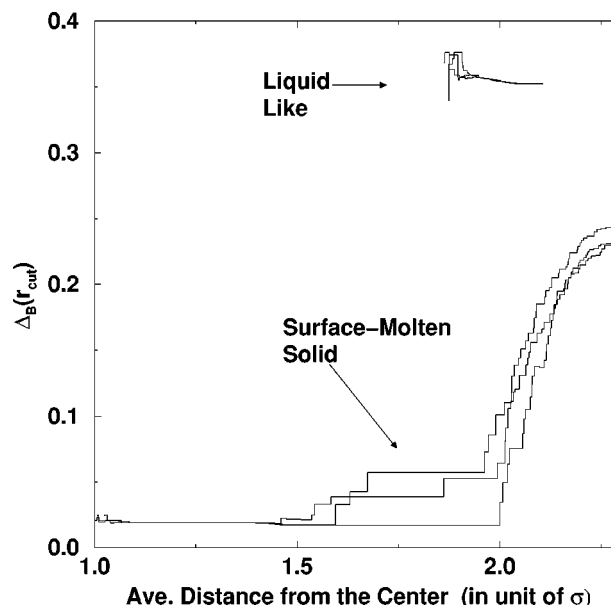


FIG. 3. As in Fig. 1 but for a cluster of 64 square-well beads at  $T^* = 0.29$ . The results of six independent runs are shown.

( $0.2\sigma < r < 2.3\sigma$ ) and those in the liquid-like phase of the homopolymer chain ( $1.3\sigma < r < 2.1\sigma$ ) (Fig. 2). This indicates that the beads in liquid-like clusters interchange positions at such a rate that they all have approximately the same average distance from the center. During the transition from the surface-molten solid to the liquid-like phase, the  $\Delta_B$  value for the whole cluster jumps from 0.2 to  $>0.35$ . If the critical value is estimated from these values, a value around 0.2 would be obtained. This value is significantly larger than  $\sim 0.1$  for the chain. In contrast, the critical value based on the core  $\Delta_B$  value for both the chain and the cluster is around 0.03. Thus, use of the core to evaluate the critical value of  $\Delta_B$  is more appropriate and more general than the use of the entire system. Unstable critical values based on the  $\Delta_B$  value for the complete finite system have been found in molecular clusters.<sup>22</sup> Whether these are also caused by surface motions requires further study.

Figure 4 compares the results of the  $\Delta_L$  parameter with those of the  $\Delta_B$  parameter for square-well clusters. It shows that the magnitude of the  $\Delta_B$  parameter for the cluster core is stable as the length of the simulation increases. However, the  $\Delta_L$  parameter does not converge. Analysis of the trajectories indicates that the interchange of beads on the surface of the cluster during the simulation leads to the error accumulations in removing rotational motions. This is because the method of removing rotational motion via minimizing the root mean-squared deviation is meaningful only if the relative locations of the beads are unchanged. In applying the Lindemann criterion to LJ clusters, Stillinger<sup>9</sup> avoided this problem by using the “returned” distance from local minima to estimate mean-squared fluctuations. Here we calculate the mean-squared fluctuations directly.

## B. System with a Morse potential

In Fig. 5, we compare  $\Delta_B(r_{\text{cut}})$  for the seven longest phase segments obtained for the surface-molten solid (SM)

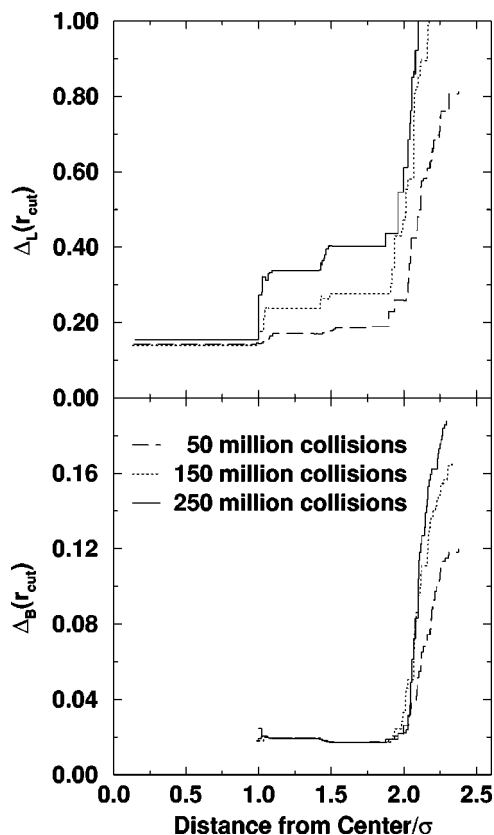


FIG. 4. Comparison of distance-dependent Lindemann and Berry parameters as a function of distance from center. Results are shown for the averages over different equilibrium simulation lengths.

phase, with that for five representative segments of the liquid-like phase. For fluctuations in the cluster core, we observe a nearly constant value  $\Delta_B = 0.048$ , with a standard deviation of less than 0.001. The value is constant over the range  $1.30\sigma \leq r_{\text{cut}} \leq 1.55\sigma$ . This range corresponds to  $N_{r_{\text{cut}}} = 13$ , which implies that the solid-like core in the SM phase

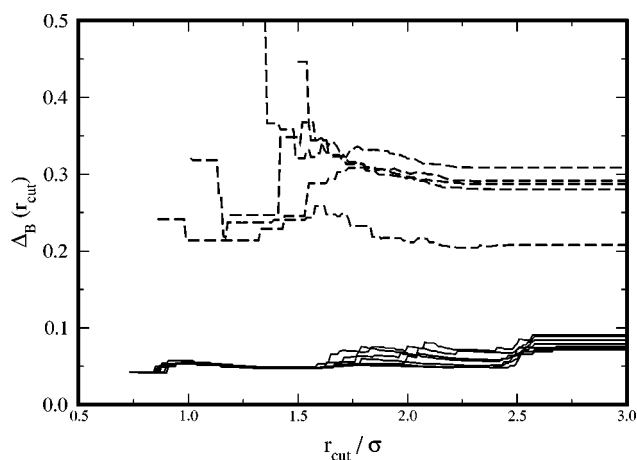


FIG. 5. The distance-dependent Berry parameter  $\Delta_B(r_{\text{cut}})$  for an isolated  $M_{64}$  cluster at  $T_{\text{melt}}^* = 0.29$ . The results for seven segments of a trajectory for the surface-melted solid phase (solid lines) and five segments of the trajectory in the liquid-like phase (dashed lines). As noted in Fig. 1, the number of particles included in the fluctuation average increases discretely with  $r_{\text{cut}}$ , causing a stepwise dependence of  $\Delta_B$  on  $r_{\text{cut}}$ . The terminal values of  $\Delta_B$  on the right-hand side of the graph represent the  $\Delta_B$  value for the entire cluster.

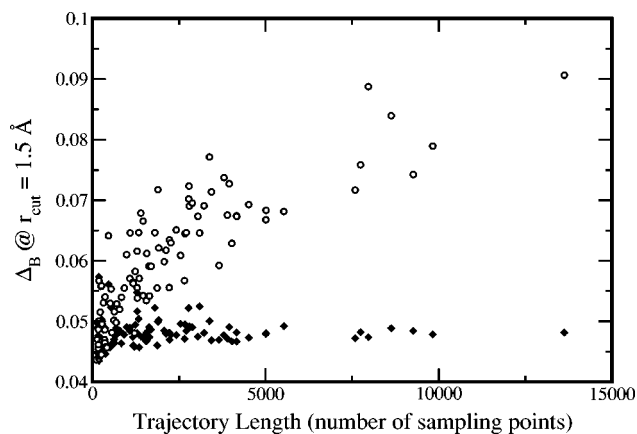


FIG. 6. The value of  $\Delta_B$  for the solid-like core (diamonds) and for the entire cluster (circles) for the surface-melted phase as a function of trajectory length.

consists of a single-shell Mackay icosahedron, the global minimum of the “magic number” cluster  $M_{13}$ . Visual inspection of quenched configurations proves this to be the case. Outside this core there is a second icosahedral shell. The full structure of the  $M_{64}$  global minimum of this cluster consists of a two-shell Mackay icosahedron (the ground state of  $M_{55}$ ) with an additional cap of nine particles at one end of the cluster, which resides at the surface in a mostly unfilled third icosahedral shell.<sup>44</sup> This geometry has consequences for the functional form and variance of  $\Delta_B(r_{\text{cut}})$  which is discussed in the following.

In contrast, the  $\Delta_B$  values for the whole cluster in its SM phase are somewhat higher, in the range 0.07–0.09. The values for both the solid-like core and the total cluster are similar to those observed in the square-well systems, with the exception that the critical  $\Delta_B$  value for  $M_{64}$  is in the upper range of the observed square-well values, and the average value is notably higher than the value of 0.03 in the latter case.

In Fig. 5, we also observe that the liquid-like phase has much higher values of  $\Delta_B$ , with a range of values 0.20–0.30 for the whole cluster, similar to the square-well values. There is much more variance in  $\Delta_B$  among liquid-like phase segments, since all atoms are undergoing diffusive motion to varying degrees. Specifically, the amount of diffusion increases directly with trajectory length, as expected. This is also true for the “molten” outer shell of the SM phase, but to a lesser extent, since only one or a few second-shell particles are excited into the third shell at any given instant, and motion on the cluster surface occurs predominantly by “hopping” diffusion.<sup>43,44</sup> Hopping motion occurs because of an effective “washboard” or “egg-crate” energy landscape for motion at the surface, due to the explicit interactions of outer-shell atoms with those in the second shell. The energy barriers on this washboard landscape greatly decrease the rate of diffusion of surface particles compared to diffusion in a pure liquid state.<sup>42</sup>

Since we are measuring  $\Delta_B$  over phase segments of varying length, we should examine whether segments of different lengths yield comparable results. In Fig. 6, we show

the values of  $\Delta_B$  both for the core and for all particles for each recorded SM phase segment. The full-cluster value clearly rises with increasing trajectory length, which is expected since the exchange of atoms in the second layer with those in the partly filled outer, most mobile layer is very slow, but each exchange adds significantly to  $\Delta_B$  for the entire cluster. In contrast, the critical core value of  $\Delta_B$  converges to a nearly constant value for trajectories over 4000 sampling points. This convergence is evidence that the longer trajectories we have obtained for the SM phase are sufficiently long to determine the critical value of  $\Delta_B$ .

We have already remarked that solid-like and SM-phase  $M_{64}$  clusters have the same underlying two-shell icosahedral structure as  $M_{55}$ . This similarity implies that  $r_{\text{cut}}$ -dependent fluctuation averages for the core (central atom plus inner shell) should be constant from a radius just outside that of the inner shell at  $r = 0.97\sigma$ , which defines the core radius, to just inside the radius of the outer shell at  $r = 1.78\sigma$ . In contrast, the plateau we have found is only about one third as broad. Furthermore, the irregular variation of  $\Delta_B$  with  $r_{\text{cut}}$  in Fig. 5 requires an explanation. We find that the cause of these irregularities is the eccentricity of the icosahedral shells about the center of mass, i.e., there is an asymmetry induced by the nine extra atoms added to the magic number of 55 atoms, which form a cap at one end of the cluster. This eccentricity produces a range of radial distances in the mass-centric picture ( $r_{\text{cut}}$  measured from the center of mass), washing out the discrete stepwise behavior expected for  $\Delta_B(r_{\text{cut}})$ .

We remedy this problem by shifting the cluster to the shell-centric picture ( $r_{\text{cut}}$  measured from the center of the icosahedral shells). This is achieved by calculating the center of mass of the innermost 55 atoms and then reevaluating the atomic coordinates with this center at the origin. (The perturbations in radial distances between the mass-centric and shell-centric pictures are small enough that the set of the innermost 55 atoms in the mass-centric picture has the same role in the shell-centric picture.) The new values for  $\Delta_B$  obtained for the shell-centric structures are compared with the original mass-centric results in Fig. 7 for a long SM phase segment. The variation in  $\Delta_B$  is now more stepwise and monotonic than before, and the expected discrete changes in  $\Delta_B$  now more stepwise and monotonic than before, and the expected discrete changes in  $\Delta_B$  now occur when  $r_{\text{cut}}$  approaches shell radii.

At first glance, the need in certain cases to take shell structure or other regular substructure into account by shifting the reference point for  $r_{\text{cut}}$  might seem to cause an ambiguous definition of the fluctuation parameters. However, in practice it is relatively easy to identify underlying symmetric substructures unambiguously from visual inspection and other data. For sufficiently large systems, the difference between shell-centric and mass-centric pictures will be insignificant. More importantly, the values of  $\Delta_B$  for the inner core and the total cluster are identical in both pictures, as shown in Fig. 7. We also observe this equivalence in our  $\Delta_{\text{EK}}$  results, and find only a very small deviation from equality for  $\Delta_L$ , which as previously noted for the square-well systems is sensitive to cluster rotation and permutation effects.

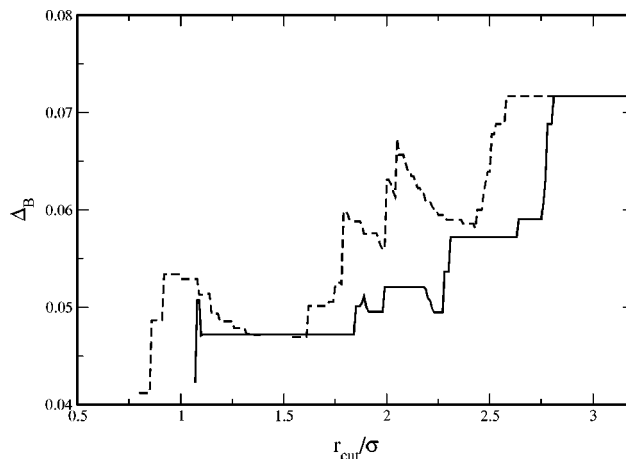


FIG. 7. Comparison of  $\Delta_B(r_{\text{cut}})$  when  $r_{\text{cut}}$  is measured from the total cluster center of mass (dashed line) and from the center of mass of the 55-particle core (solid line). The latter reference point for  $r_{\text{cut}}$  gives a clearer picture of the dependence of fluctuation parameters on the cluster geometry.

In Fig. 8 we compare the Lindemann parameter to the Berry parameter, as done for the square-well cluster in Fig. 4. We find, as was true in the square-well case, that the core  $\Delta_B$  remains stable for phase segments of varying lengths, while  $\Delta_L$  increases with segment length, even for the core region. Hence, as with the square-well potentials,  $\Delta_B$  is preferred over  $\Delta_L$  as a critical fluctuation parameter for the more realistic Morse potential.

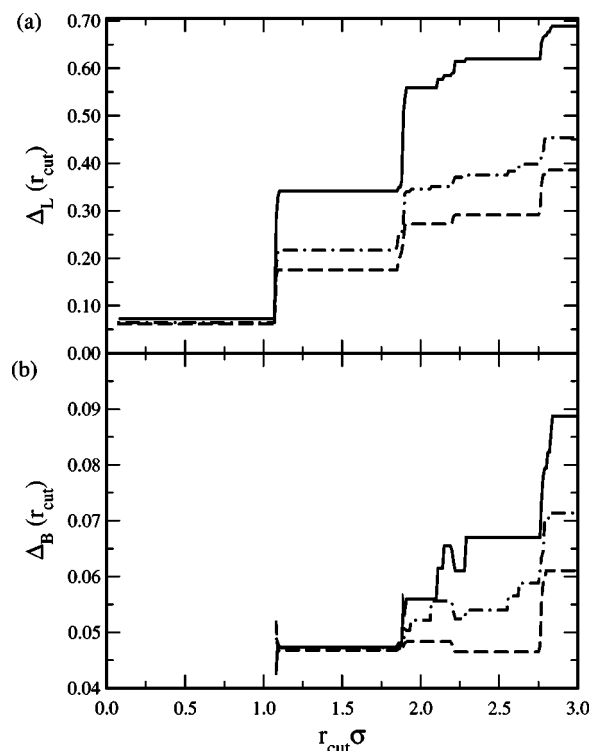


FIG. 8. Comparison of (a) Lindemann and (b) Berry parameters averaged over trajectory lengths of 4000 (dashed line), 60 000 (dotted-dashed line), and 8000 (solid line) sampling points.

#### IV. CONCLUSIONS

We have shown that the critical value for melting the distance-fluctuation criterion  $\Delta_B$  ( $\Delta_{EK}$ ) is around 0.03–0.05, a value that is significantly smaller than the critical value of the Lindemann criterion (0.1–0.15). The difference is not unexpected due to the fact that the former is based on relative atomic motions while the latter is based on individual atomic fluctuations. Correlated atomic motions in solid decrease the magnitudes of relative fluctuations with respect to the magnitudes of individual atomic fluctuations. The distance-based criterion has one immediate, clear advantage over the mean-position-based (Lindemann) criterion: the latter requires one to remove all the overall rotation of the system, which is a technically cumbersome task.<sup>45</sup>

The results of comparisons of the distance-dependent  $\Delta_L$ ,  $\Delta_{EK}$ , and  $\Delta_B$  parameters for the 64-particle Morse cluster are similar to those observed for the square-well systems. Specifically, we have shown that the criterion based on interparticle distances with a distance cutoff from a reference point avoids the complication arising from dynamic heterogeneity between core and surface.

Although the critical values of the distance-dependent fluctuation parameters can generally be obtained by choosing the center of mass as the reference point for the radial distance cutoff, we find that the structural dependence of these parameters is better captured for  $M_{64}$  by measuring this distance from the center of its icosahedral shells. In general, redefining the radial distance to accommodate specific underlying geometric symmetries may potentially aid in the extension of distance fluctuation diagnostics to nonspherically symmetric systems, such as those with cylindrical or planar symmetry.

The results from a square-well cluster are very similar to those from a square-well homopolymer, indicating that chain connectivity does not alter the liquid–solid transition, at least for a freely jointed chain.

In conclusion, we find that the distance-fluctuation criterion is likely to be the criterion of choice for studying phase changes in finite disordered systems, because it is stable, dimensionless, and easy to evaluate.

#### ACKNOWLEDGMENTS

This work was supported by grants from the National Science Foundation and a grant from Pittsburgh Supercomputing Center to M.K. Y.Z. was a National Institutes of Health Postdoctoral Fellow. He is now supported in part by a grant from HHMI to SUNY Buffalo and by the Center for

Computational Research and the Keck Center for Computational Biology at SUNY Buffalo. K.D.B. acknowledges support by a Fellowship from the Program in Mathematics and Molecular Biology at the Florida State University, with funding from the Burroughs Wellcome Fund Interfaces Program.

- <sup>1</sup>F. A. Lindemann, *Phys. Z* **11**, 609 (1910).
- <sup>2</sup>J. P. Hansen and L. Verlet, *Phys. Rev.* **184**, 151 (1969).
- <sup>3</sup>H. Löwen, T. Palberg, and R. Simon, *Phys. Rev. Lett.* **70**, 1557 (1993).
- <sup>4</sup>F. H. Stillinger, *Science* **267**, 1935 (1995).
- <sup>5</sup>H. Löwen, *Phys. Rep.* **237**, 249 (1994).
- <sup>6</sup>J. H. Bilgram, *Phys. Rep.* **153**, 1 (1987).
- <sup>7</sup>D. A. Young and B. J. Alder, *J. Chem. Phys.* **60**, 1254 (1974).
- <sup>8</sup>E. J. Meijer and D. Frenkel, *J. Chem. Phys.* **94**, 2269 (1991).
- <sup>9</sup>F. H. Stillinger and D. K. Stillinger, *J. Chem. Phys.* **93**, 6013 (1990).
- <sup>10</sup>Y. Zhou, M. Karplus, J. M. Wichert, and C. K. Hall, *J. Chem. Phys.* **107**, 10691 (1997).
- <sup>11</sup>Y. Zhou and M. Karplus, *Proc. Natl. Acad. Sci. U.S.A.* **94**, 14429 (1997).
- <sup>12</sup>Y. Zhou, D. Vitkup, and M. Karplus, *J. Mol. Biol.* **285**, 1371 (1999).
- <sup>13</sup>R. D. Eppers and J. Kaelberer, *Phys. Rev. A* **11**, 1068 (1975).
- <sup>14</sup>R. D. Eppers and J. Kaelberer, *J. Chem. Phys.* **66**, 5112 (1977).
- <sup>15</sup>J. B. Kaelberer and R. D. Eppers, *J. Chem. Phys.* **66**, 3233 (1977).
- <sup>16</sup>R. S. Berry, T. L. Beck, H. L. Davis, and J. Jelinek, *Adv. Chem. Phys.* **70B**, 75 (1988).
- <sup>17</sup>D. D. Frantz, *J. Chem. Phys.* **102**, 3747 (1995).
- <sup>18</sup>D. J. Wales and I. Ohmine, *J. Chem. Phys.* **98**, 7245 (1995).
- <sup>19</sup>L. S. Bartell and F. J. Dulles, *J. Phys. Chem.* **99**, 17107 (1995).
- <sup>20</sup>C. Seko and K. Takatsuka, *J. Chem. Phys.* **104**, 8613 (1996).
- <sup>21</sup>D. Wright and M. S. Elshall, *J. Chem. Phys.* **105**, 11199 (1996).
- <sup>22</sup>K. E. Kinney, S. M. Xu, and L. S. Bartell, *J. Phys. Chem.* **100**, 6935 (1996).
- <sup>23</sup>A. Dawid and Z. Gburski, *J. Mol. Struct.* **410**, 507 (1997).
- <sup>24</sup>V. V. Nauchitel and A. J. Pertsin, *Mol. Phys.* **40**, 1341 (1986).
- <sup>25</sup>R. S. Berry, *Microscale Thermophys. Eng.* **1**, 1 (1997).
- <sup>26</sup>H. E. Kunz and R. S. Berry, *Phys. Rev. Lett.* **71**, 3987 (1993).
- <sup>27</sup>Y. Zhou, C. K. Hall, and M. Karplus, *Phys. Rev. Lett.* **77**, 2822 (1996).
- <sup>28</sup>W. Kabsch, *Acta Crystallogr., Sect. A: Cryst. Phys., Diffr., Theor. Gen. Crystallogr.* **32**, 922 (1976).
- <sup>29</sup>D. T. Mainz and R. S. Berry, *Mol. Phys.* **88**, 709 (1996).
- <sup>30</sup>P. A. Braier, R. S. Berry, and D. J. Wales, *J. Chem. Phys.* **93**, 8745 (1990).
- <sup>31</sup>P. K. Doye, D. J. Wales, and R. S. Berry, *J. Chem. Phys.* **103**, 4234 (1995).
- <sup>32</sup>J. P. K. Doye and D. J. Wales, *J. Phys. B* **29**, 4859 (1996).
- <sup>33</sup>J. P. K. Doye and D. J. Wales, *J. Chem. Soc., Faraday Trans.* **93**, 4233 (1997).
- <sup>34</sup>M. A. Miller, J. P. K. Doye, and D. J. Wales, *J. Chem. Phys.* **110**, 328 (1999).
- <sup>35</sup>P. Labastie and R. L. Whetten, *Phys. Rev. Lett.* **65**, 1567 (1990).
- <sup>36</sup>H.-P. Cheng, X. Li, R. L. Whetten, and R. S. Berry, *Phys. Rev. A* **46**, 791 (1992).
- <sup>37</sup>S. M. Kast, K. Nicklas, H.-J. Baer, and J. Brickmann, *J. Chem. Phys.* **100**, 566 (1994).
- <sup>38</sup>S. M. Kast and J. Brinkmann, *J. Chem. Phys.* **104**, 3732 (1996).
- <sup>39</sup>D. S. Sholl and K. A. Fichtorn, *J. Chem. Phys.* **106**, 1646 (1997).
- <sup>40</sup>F. H. Stillinger and T. A. Weber, *Phys. Rev. A* **25**, 978 (1982).
- <sup>41</sup>Y. Imry, *Phys. Rev. B* **21**, 2042 (1980).
- <sup>42</sup>H.-P. Cheng and R. S. Berry, *Phys. Rev. A* **45**, 7969 (1992).
- <sup>43</sup>R. E. Kunz and R. S. Berry, *Phys. Rev. E* **49**, 1895 (1994).
- <sup>44</sup>J. P. K. Doye and D. J. Wales, *J. Chem. Phys.* **102**, 9673 (1995).
- <sup>45</sup>Y. Zhou, M. Cook, and M. Karplus, *Biophys. J.* **79**, 2902 (2000).